

# Adaptive Linearization Through Narrowband Feedback

Alexander N. Lozhkin

Fujitsu Limited, YRP R&D Center  
5-5 Hikari-no-Oka, Yokosuka, Japan  
[a.n.lozhkin@jp.fujitsu.com](mailto:a.n.lozhkin@jp.fujitsu.com)

Michiharu Nakamura

Fujitsu Limited, YRP R&D Center  
5-5 Hikari-no-Oka, Yokosuka, Japan

**Abstract**— An adaptive predistorter (PD) is an effective technique to compensate for the nonlinear distortion of power amplifiers. To enable broadband communications, the bandwidth of communication systems has had to continuously increase. With these increases in bandwidth, frequency distortions due to limitations in the bandwidth of the PD's building blocks can no longer be ignored. Such distortions are important factors that define a PD's linearization performance. In this study, we investigated the adaptive PD performance degradation caused by bandwidth restrictions in the feedback (FB) path. Employing a newly proposed graphical approach which we confirmed by computer simulations. We show that achieving PD linearization with narrowband FB strongly depends on the PD's architecture and the FB path bandwidth. Finally, we make practical recommendations regarding the implementation of adaptive PDs having memoryless and memory polynomial architectures that depend on the available FB path bandwidth.

**Keywords**— DPD, baseband predistortion, linearization, power amplifier, memory effect.

## I. INTRODUCTION

In recent years, there has been growing interest in linearization through the use of predistortion [1-5]. The predistortion technique in its simplest memoryless form has been successfully implemented for the linearization of high power amplifiers (HPAs) for relatively narrowband 2G and 2.5G communication systems. In order to provide broadband communications, the signal bandwidth in existing 3G and upcoming 4G communication systems has continuously increased. Therefore, as the bandwidth of the transmitted signal increases, there arises a memory effect in HPAs. In [5], it is shown that the performances of the simple memoryless PD, which do not consider memory effects, are severely degraded as the bandwidth of the input signal increases.

In order to overcome such problems, several new predistorter architectures based on the Volterra series have been proposed [1-5]. In the most cited studies, ideal signaling conditions are assumed, i.e., the conditions when there is no signal bandwidth restriction in the PD's building blocks. Thus, the linearization capabilities of the linearizers proposed in [1-5] remain unclear for practical cases involving PDs having frequency limited building blocks.

The main objective of this investigation is to investigate the effects of the continuous growth in transmitted signal

bandwidths. As a general rule of thumb, the  $k^{\text{th}}$  order of a power amplifier's (PA) nonlinearity causes the appearance of a parasitic component occupying  $k$  times the bandwidth of the input signal. In modern 4G communication systems such as WiMAX or LTE, which account for inter-modulation products in the HPA output, the FB bandwidth for sample-by-sample comparison has already exceeded the 100 MHz limit. For signals having such wide bands, the frequency distortion due to the passband bandwidth limitation in the PD's building blocks can no longer be ignored. These frequency distortions are therefore important defining factors for a PD's linearization performance.

In adaptive PD systems, it is necessary to have a FB path. Most RF and baseband circuits have limited bandwidth and the implementation of such frequency selective circuits is inevitable, as they are present in both direct and FB paths of the adaptive PD, regardless of the architecture of a specific PD. Due to the negative FB properties, the distortions that originated in the FB path define the total system distortion [7]. These distortions are translated directly into the HPA output. In this paper, we therefore restrict our discussion signal distortion in the PD's narrowband FB path.

Another reason to restrict our investigation to distortions in the FB path is directly related to the PD's production cost. The high-speed ADCs in the FB path tend to be the most expensive component in transmitters with PDs. A less costly alternative is to adopt a PD that uses only narrowband FB.

In this paper, with semi-analytical graphical approaches and with the aid of computer simulations, we have evaluated the level of the linearization performance degradation as a function of the PD FB path bandwidth. We aim to determine whether the high complexity memory polynomial (M-P) PD provides better linearization than the memoryless (M-L) PD in the case of narrowband FB. The remainder of the paper is organized as follows. Section II describes the model of an HPA that has a memory effect that was used during the simulation. Here, we discuss the indirect learning structure for PDs and give a brief mathematical background for polynomial regression analysis. Section III introduces the concept of the equivalent disturbance power that is used for the analysis of PD performance degradation. Section IV describes the proposed semi-analytical graphical approach that predicts the

spectral regrowth caused by frequency restrictions in the PD FB path. We also presented the simulation results obtained for both M-L and M-P adaptive linearization through the narrowband FB path. We show that the degradation levels that were predicted with the graphical approach agree well with the data obtained from the direct computer simulations over a wide range of FB bandwidths. Finally, we make practical points regarding the implementation of the M-P and M-L polynomial PDs for the linearization of HPA through narrowband FB.

## II. SYSTEM MODEL

### A. HPA Model

As mentioned above, as the bandwidth of the transmitted signal increases, a memory effect is noticed in HPAs. The expression “having memory” implies that the output of the HPA depends on the system response for both the input signal amplitude and the signal envelope frequency. This is the reason for the memory effect in HPAs to be most pronounced for wideband signals with high peak-to-average power ratio (PAPR) such as for multiple W-CDMA, WiMAX or LTE. The baseband behavior of HPAs that have the memory effect can be described using a complex M-P model [1, 5]. During the simulations, the HPA was modeled as the *odd-order* M-P of order  $K = 5$  and memory depth  $Q = 3$ , as shown in equation (1).

$$y(n) = \sum_{k=1}^K \sum_{q=0}^Q c_{kq} \cdot z(n-q) \cdot |z(n-q)|^{k-1}, \quad (1)$$

### B. Predistorter With Indirect Learning

First, we briefly review the M-P linearization that follows the treatment in [1]. Figure 1 shows the indirect learning architecture that is used for PD identification.

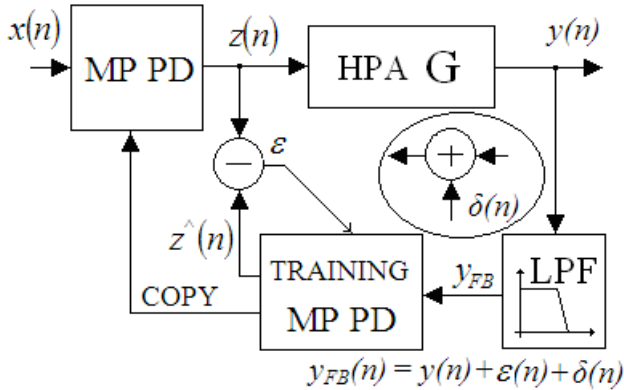


Figure 1. System Model. Indirect Learning (PD)

The objective of the linearizer is to identify the transformation of the signal ( $z(n) = \text{HPA}^{-1}(x(n))$ ) that, together with nonlinear HPAs, will result in an identity system that produces the signal of interest without distortions at the output of the HPA, i.e.,  $y(n) = x(n)$ . Using this approach, two identical M-P systems (denoted in Figure 1 as PD) are used for

training and predistortion. The FB path comprises the low-pass filter (LPF) that limits the FB path bandwidth and a training PD that has an input of  $y_{FB}(n)$  and an output of  $\hat{z}(n)$ . The actual predistorter is an exact copy of the training predistorter, in that it has  $x(n)$  as its input and  $z(n)$  as its output.

We assume that the bandwidth of the LPF placed in the PD FB path is sufficiently wide such that the LPF does not introduce any significant distortion into the PD's FB signal ( $y(n)$ ) from the HPA output. The exact influence of the LPF (that is placed in the FB path) on the PD linearization performances will be discussed in Sections III and IV. Therefore, the following approximation becomes valid:  $y_{FB}(n) = y(n)$ . The M-P predistorter can be considered to be similar to [1-2], and is given as:

$$z(n) = \sum_{k=1}^K \sum_{q=0}^Q a_{kq} \cdot x(n-q) \cdot |x(n-q)|^{k-1} \quad (2)$$

where  $a_{kq}$  are the unknown complex M-P predistorter coefficients,  $x(n)$  represents the transmitting signal samples at a discrete time  $n$ .

Ideally, after initialization through indirect learning, at convergence we should have  $z(n) = \hat{z}(n)$ , or in the matrix form [1]:  $Z = Y \cdot A$  (3)

where:  $y_{kq}(n) = y(n-q) \cdot |y(n-q)|^{k-1}$  ;  
 $Z = [z(0), \dots, z(N-1)]^T$  ,  $Y = [Y_{10}, \dots, Y_{KQ}]$  ,  
 $Y_{kq} = [y_{kq}(0), \dots, y_{kq}(N-1)]^T$  ,  $A = [a_{10}, \dots, a_{KQ}]^T$  , and  
 $N$  is the number of available data samples  $n$ .

The error term is not explicitly present in the expression (3). Therefore, to investigate the influence of the linearization error, we employed the linear regression approach [9].

### C. Polynomial Regression

The polynomial regression fits a nonlinear relationship between the value of  $y_{FB}(n)$  and the corresponding conditional mean of  $\hat{z}(n)$  (Figure 1). Because  $\hat{z}(n)$  is linear with respect to the unknown parameters  $a_{kq}$  (2), these unknown parameters can be estimated by a simple least-square method by treating  $y_{FB}, y_{FB}^2, \dots, y_{FB}^{K-1}$  as being distinct independent variables in a multiple regression model. This is so because usually, only the approximate solution for the polynomial regression can be obtained. There is an unobserved random error  $\varepsilon(n)$  (known as a disturbance term) with mean zero and is shown in (4).

$$\text{Therefore, } \varepsilon(n) = z(n) - \hat{z}(n) \quad (4)$$

The regression results were less than satisfactory when the independent variables were correlated and the disturbance term is not independent and identically distributed (i.i.d.) [8]. For the relatively wideband LPF that is assumed above, the  $\varepsilon(n)$  error is an i.i.d. random variable. Given  $y(n)$  and  $z(n)$ , the PD's training task is to identify the parameters  $a_{kq}$  of the M-P

PD (2) which yields the PD. The algorithm converges when the error energy  $\|\varepsilon(n)\|$  is minimized. Thus, in the polynomial regression model, we have:

$$z(n) = z^{\wedge}(n) + \varepsilon(n) \quad (5)$$

$$z(n) = \sum_{k=1}^K \sum_{q=0}^Q a_{kq} \cdot y_{kq}(n) + \varepsilon(n) \quad (6)$$

Equation (6) can be expressed using a pure matrix notation that is similar to (3), and is given as:

$$Z = Y \cdot A + \varepsilon \quad (7)$$

The vector of the estimated polynomial regression coefficients  $a_{kq}$  using the least-squares solution for (7) is:

$$A = (Y^T \cdot Y)^{-1} \cdot Y^T \cdot Z \quad (8)$$

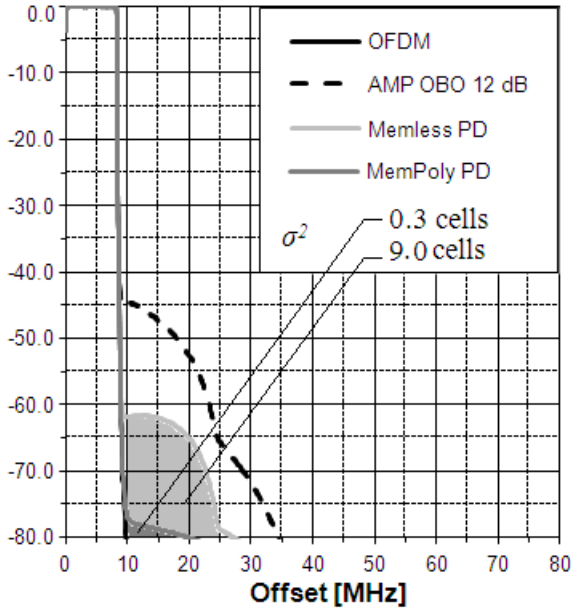


Figure 2. Disturbance noise power  $\sigma_o^2$  estimation.

#### D. LPF Models For PD's Narrowband FB Path

In order to simulate the bandwidth restriction in the PD's FB path, a LPF with an adjustable cut-off frequency was included in the FB path as is shown in Figure 1. By preselecting the LPF bandwidth, it was possible to control the extent of the frequency domain distortion in the PD's FB signal during the simulations. Three LPFs with the bandwidths that are denoted as LPF-1, LPF-1.5 and LPF-2 were selected. The indices after "LPF" indicate the normalized LPF bandwidth, which is the LPF bandwidth  $\Delta f$  that is normalized to the bandwidth of the transmitting signal  $x(n)$ . Therefore, the LPFs used during the simulations have bandwidths  $\Delta f$  that are equal to 20, 30, and 40 MHz, respectively.

### III. DISTURBANCE TERM EQUIVALENT POWER

#### A. Out-Of-Band Disturbance Power Terms

The disturbance term  $\varepsilon(n)$  that is used in (7) is responsible for the residual linearization error. i.e., it is the reason for the difference between the spectrum of the HPA output signal

after linearization  $y(n)$  and the spectrum of the originally transmitted signal  $x(n)$ . Depending on the occupied frequency range, the disturbance term  $\varepsilon(n)$  can be separated into two parts, which are responsible for the in-band  $\varepsilon_I(n)$  and out-of-band  $\varepsilon_O(n)$  spectrum distortions. Therefore,  $\varepsilon(n) = \varepsilon_I(n) + \varepsilon_O(n)$ . Next, we estimate the equivalent power  $\sigma_o^2$  of the disturbance term  $\varepsilon_O(n)$  that is responsible for the out-of-band emission. In [10], based on the Taylor series expansion, we obtained the expression for  $Y(f)$ , which is the PSD signal at the nonlinear HPA output.

$$Y(f) = K_1 S_X(f) + K_2 S_X(f) \otimes S_X(f) S_X(-f) + K_3 S_X(f) \otimes S_X(f) \otimes S_X(-f) S_X(-f) \quad (9)$$

In (9),  $S_X(f)$  is an input having a complex envelope power

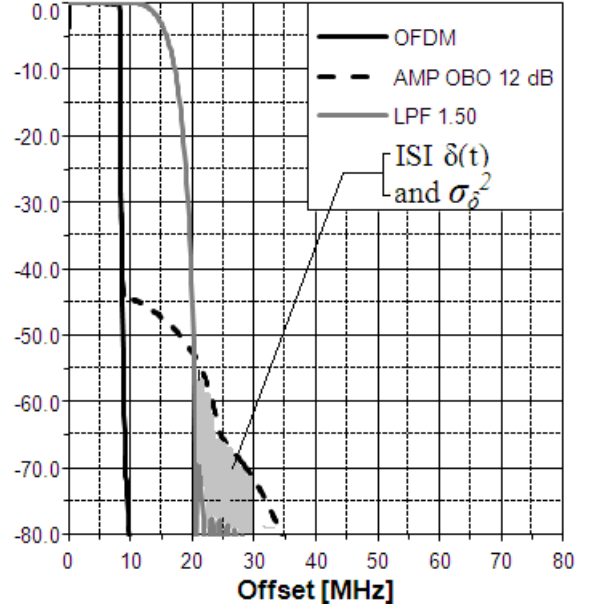


Figure 3. The equivalent power  $\sigma_o^2$  estimation.

spectral density, and  $\otimes$  refers to the convolution. The relationships between the coefficients  $K_1$ ,  $K_2$ , and  $K_3$  in (9) and the HPA model coefficients  $c_k$  in (1) are described as [10]:

$$K_1 = |c_1|^2 + 4\Re(c_1 \cdot c_3^*)P_{in} + 4|c_3|^2 P_{in} + 12\Re(c_1 \cdot c_5^*)P_{in}^2 + 24\Re(c_3 \cdot c_5^*)P_{in}^2 + 36|c_5|^2 P_{in}^4$$

$$K_2 = 2|c_3|^2 + 24\Re(c_3 \cdot c_5^*)P_{in} + 72|c_5|^2 P_{in}^2 ; K_3 = 12|c_5|^2$$

where  $\Re(\bullet)$  denotes the real part.

According to Parseval's theorem, the equivalent power of the out-of-band spectrum for the positive frequencies is:

$$\sigma_o^2 = \int_{\Delta f/2}^{\infty} |Y(f)|^2 df = 1/2 \int_0^{\infty} |\varepsilon_O(t)|^2 dt \quad (10)$$

The integral (10) can be computed numerically. However, it is easy to estimate the equivalent power  $\sigma_o^2$  based on the PSDs

shown in Figure 2, without performing extensive numerical integration. The PSD shown in Figure 2 has the dimension [Watt/Hz], and the area under the PSD plot therefore represents the signal power. The power of the disturbance term  $\varepsilon_0(n)$  is equal to the square under the PSD's curves in the out-of-band area. Thus, in the case of the M-L PD, the equivalent power  $\sigma^2$  equals approximately 9 cells (cells filled with the dark solid color). Meanwhile, for the M-P PD,  $\sigma_0^2$  occupies only 0.3 cells. Therefore, the difference between the out-of-band emissions that can be realized with the M-L and M-P PDs is 14.8 dB. This result agrees well with the PSD plots presented in Figure 2. Here, we assumed that for the PSD plots, a single cell is constructed by the intersection of the axes' grid lines.

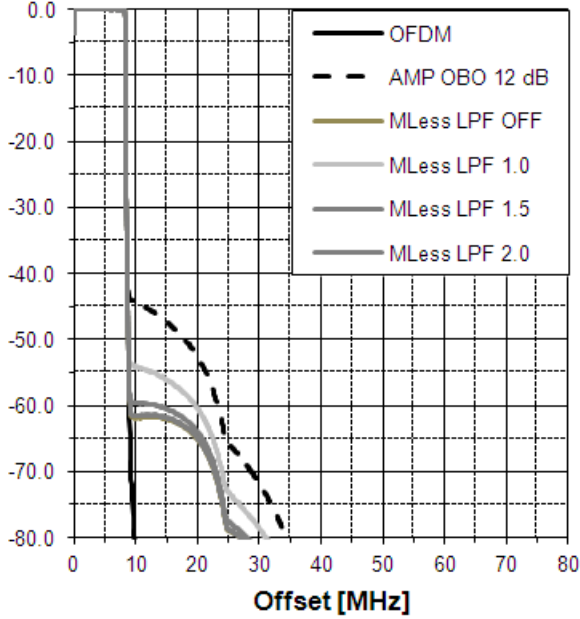


Figure 4. Effectiveness of the M-L PD, OBO 12 dB.

#### B. Concept Of the Equivalent Disturbing Noise Power

For further analysis of the PD performance degradation, we employed the equivalent LPF schema, as shown in the circle in Figure 1. Thus, the LPF has been replaced with some equivalent external interference (ISI)  $\delta(n)$  source. This interference  $\delta(n)$  can be treated as *colored noise* having an equivalent power  $\sigma_\delta^2$  that is equal to the square under the PSD curves in the LPF stop-band in Figure 3. For the linear regression analysis described in Section II, the LPF that is placed in the FB path increases the disturbance term in (6) from  $\varepsilon(n)$  to  $\varepsilon(n) + \delta(n)$ . This increase results in an increase in the out-of-band spectrum level. The equivalent power of the disturbance term  $\delta(n)$  for the positive frequencies can be calculated as:

$$\sigma_\delta^2 = \int_{\Delta f/2}^{\infty} |Y(f)|^2 df. \quad (11)$$

## IV. SIMULATION RESULTS

### A. PD Without Frequency Restrictions

The linearization performances of a PD with an indirect learning architecture (8) have been investigated using computer simulation tools. An HPA that obeys the M-P model (1) described in [1] with output backoff (OBO) 12 dB was used during the simulations. The baseband input  $x(n)$  is an OFDM signal with 2048 subcarriers and an RF bandwidth  $\Delta F$  that is equal to 20 MHz. The spectrum of the original signal is shown in Figure 3 on the plot marked OFDM. Identification of the PD is carried out based on 8,000 data samples ( $N = 8000$ ). In the absence of any precautions, the HPA's output signal has a high level of the out-of-band spectrum, as shown in Figure 3

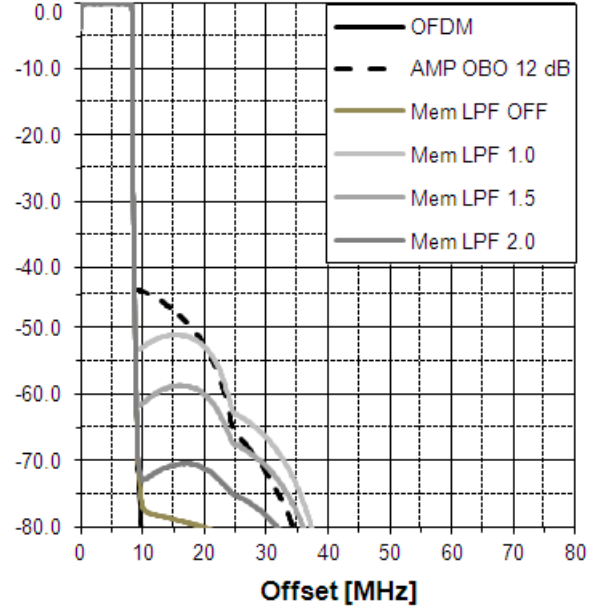


Figure 5. Effectiveness of the M-P PD, OBO 12 dB.

by dotted line marked as “AMP OBO 12 dB”. Next, we compare the power spectral density (PSD) of the input and output signals to evaluate the effectiveness of the predistorter. The PSD for the HPA output signal obtained with the M-L predistorter (2) using  $K = 5$  and  $Q = 0$ , is demonstrated in Figure 2 using the Memless PD plot. Alternatively, PSDs were obtained with the M-P PD ( $K = 5$ ,  $Q = 3$ ) and marked as MemPoly PD. It is found that for the “ideal” signaling conditions the M-P PD significantly overperforms the M-L PD. Next, we examine whether there will be the same tendency to commit in the case of the narrowband FB path.

### B. The PD Performance Degradation Prediction

Here, we proposed a new graphical approach for estimation of PD performance degradation caused by narrowband FB paths. As mentioned above, the disturbance term  $\varepsilon(n)$  is already present in the PD solution (6). For most practical cases, HPAs can be treated as very wideband devices. Therefore, there is a low correlation of  $\varepsilon(n)$  between the samples, and it can be treated as an i.i.d. variable with zero mean and equivalent noise power  $\sigma_\varepsilon^2$ . This is the main reason



for the good results achieved by linearization based on the polynomial linear regression theory, even when HPA is described as a nonlinearity with memory [8, 9].

The inclusion of a LPF into the PD's FB path introduces an additional colored noise  $\delta(n)$ , and therefore increases the total noise power of the disturbance in (6). The equivalent power  $\sigma_\delta^2$  of the  $\delta(n)$  level can be estimated using (11) or by the calculation area under the PSD plot for the HPA output signal in the LPF stop-band frequency range (Figure 3). As an example, Figure 3 shows that the area that corresponds to the equivalent power of  $\delta(n)$  from LPF-1.5, occupies approximately 7 cells. With the numerical data extracted from the PSD plots in the previous section, the total noise power  $\sigma_\theta^2 + \sigma_\delta^2$  after including the LPF into the M-L PD FB path is increased for  $10 \cdot \log((\sigma_\theta^2 + \sigma_\delta^2)/\sigma_\theta^2)$  or  $10 \cdot \log((9+7)/9) = 2.5$  dB. In the case of the M-P PD, the LPF-1.5 in the FB path increases the disturbance term power by  $10 \cdot \log((0.3+7)/0.3) = 13.85$  dB, which is significantly higher than the results obtained for the M-L PD. In particular, the initial low level of the  $\sigma_\theta^2$  for M-P PD defines its high level of degradation as well as its high sensitivity to the frequency restrictions in the FB path.

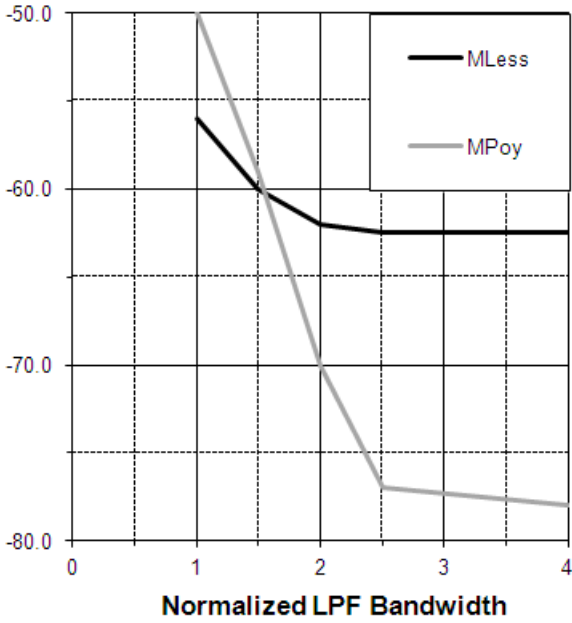


Figure 6. The out-of-band Level [dB].

For most practical LPFs (i.e., anti-aliasing analog-to-digital-converter LPFs) [3] with normalized bandwidth  $\Delta f/\Delta F \geq 1$ , the spectrum for the disturbance term  $\delta(n)$  occupies only the out-of-band frequency range. Therefore, the disturbance term  $\delta(n)$  does not significantly change the PSD shape and is translated directly into the out-of-band spectrum level. Thus, the additional disturbance term  $\delta(n)$  will increase the level of the out-of-band component by 2.5 dB for M-L and by 13.85 dB for the M-P PDs, respectively. These predictions for the out-of-band spectrum levels are very close to the results obtained with the aid of computer simulations shown in

Figures 4 and 5 and partially depicted in Figure 7 as PD performance degradation. Similar calculations for LPF-1 and LPF-2 predict PD's performance degradations of 4.1/0.65 dB for M-L and 17.3/7.5 dB for M-P PDs, respectively. The overly optimistic prediction for the M-P PD's performance degradation in the case of LPF-1 can be explained by the fact that the narrowband LPF-1 produces a highly-correlated noise  $\delta(n)$ . This highly-correlated noise dominates the low-correlated white Gaussian noise-like disturbance term  $\varepsilon(n)$ . Therefore, the simple i.i.d. Gaussian noise disturbance model for (6) was not successful and the polynomial regression obtained for the uncorrelated Gaussian noise was no longer valid [8].

In general, until the residual disturbance term  $\varepsilon(n)$  dominates against the inter-symbol interference (ISI)  $\delta(n)$  from the LPF (i.e., when  $\varepsilon(n) > \delta(n)$ ), there is no significant error in the prediction of the M-L PD performance degradations. For example, in the case of relatively wideband LPF-2, the graphical calculations and direct computer simulations described above both give M-L PD performance degradations less than 1 dB. An example involving the LPF-1.5 can be considered to be a benchmark case where the residual disturbance term  $\varepsilon(n)$  in (6) and the ISI from the LPF

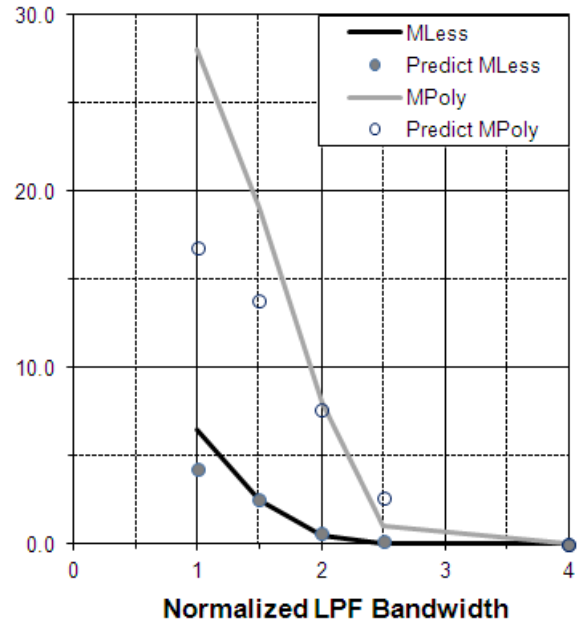


Figure 7. PD Performance Degradation [dB].

$\delta(n)$  have approximately the same power level.

Thus, the total power of the disturbance noise  $\sigma_\theta^2 + \sigma_\delta^2$  is doubled and translates into a PD performance degradation of 3 dB. In this case, both the graphical approach and the direct computer simulations result in the same 2.5 dB PD performance degradation level. The implementation of the narrowband LPF-1 increases the ISI from the LPF  $\delta(n)$  against the i.i.d. residual disturbance term  $\varepsilon(n)$ . For FBs with such a narrow band, the PD performances deteriorate significantly and the results obtained with the aid of the computer

simulation give a more severe degradation that can be predicted using the proposed graphical approach in the i.i.d. disturbance term  $\varepsilon(n) + \delta(n)$  assumption.

### C. Linearization Performances For Memoryless VS Memory Polynomial Predistorters

In this section, we summarize the effect of LPFs placed into the PD's FB path on the linearization performances of the M-L and M-P PDs. The maximum level of the out-of-band spectrum after linearization was selected as a criterion of linearization quality. Figure 6 shows the achievable levels of the out-of-band spectrums for M-L and M-P PDs as a function of the PDs FB path LPF bandwidths. Figure 7 depicts the PDs performance degradation as a function of the normalized LPF passband bandwidth for M-L and M-P PDs, respectively. In these figures, the plots denoted as "MLess" correspond to the M-L PD, while the plots denoted as "MPoly" correspond to the M-P PD. The circles in Figure 7 show the predicted values that were obtained using the proposed graphical approach for PD performance degradation for both M-L and M-P PDs. This figure shows that the predicted values for both PD architectures agree well with the results obtained from the direct computer simulations.

One interesting fact regarding M-L and M-P PD implementation is that, as shown in Figure 7, until the normalized LPF passband bandwidth do not exceed value of 1.5, the M-L PD provides better spectrum regrowth reduction than the M-P PD, even if the HPA is obeying the M-P model (1). In contrast, the superiority of adaptive linearization with the M-P PD over linearization with the M-L PD is more pronounced for relatively wide band FB paths. Finally, the implementation of the high cost and high complexity M-P PD without considering the FB path bandwidth does not automatically guarantee better linearization performances. For FB paths that have relatively narrow bands, a simple, low complexity polynomial PD can provide better performances than high complexity M-P PDs.

## V. CONCLUSION

In this paper we have investigated the adaptive PD linearization performance degradation caused by bandwidth restrictions of the FB path. Results for PD degradation due to narrowband FB paths that were obtained using the proposed graphical approach agree well with results obtained directly

with the aid of computer simulations. According to the obtained results, the PDs ability to linearize an HPA deteriorates as the FB path bandwidth narrows, because the narrowband FB introduces additional distortions during learning. However, the absolute values for the PDs linearization performance degradation depend strongly on the specific type of PD and the FB path bandwidth. Thus, the PD with the M-P architecture is more sensitive to FB path bandwidth restrictions than the M-L polynomial PD. The linearization capability of the M-P PD deteriorates quickly as the FB path bandwidth decreases. Meanwhile, the M-L PD provides stable linearization performances for a wide range of FB path bandwidths. Moreover, in the cases of relatively narrowband FB, PDs that have the low-complexity M-L architecture provide better spectral regrowth reduction than a very complex M-P PD. Generally, there is a classical tradeoff between the linearization performances, PD complexity and the available FB path bandwidth.

## REFERENCES

- [1] Lei Ding et al., "A Robust Digital Baseband Predistorter Constructed Using Memory Polynomials," IEEE Transaction on Communications, vol. 52, no 1, pp.159-165, Jan. 2004.
- [2] J. Kim and K. Konstantinou, "Digital predistortion of wideband signals based on power amplifier model with memory," Electron Lett., vol. 37, no. 23, pp. 1417 – 1418, Nov. 2001.
- [3] Weiyun Shan, Lars Sundstrom, "Effects of Anti-Aliasing Filters in FB Path of Adaptive Predistortion," IEEE MTT-S Int. Microwave Symp. Dig., vol. 2, pp. 469-472, 2002.
- [4] L. Gan and E. Abd-Elrady, "Digital Predistortion of Memory Polynomial Systems using Direct and Indirect Learning Architectures," ACTA Press, Australia..
- [5] F. M. Ghannouchi, O.Hammi, "Behavioral modeling and predistortion," IEEE Microwave Magazine, vol.10, no. 7, pp.52-64, Dec. 2009.
- [6] P. Draxler et al., "Memory Effect Evaluation and Predistortion of Power Amplifiers," IEEE MTT -S Int. Microwave Symp. Dig. pp.1549-1552, June 2005.
- [7] W. McC. Siebertt, "Circuits, Signals, and Systems," MIT Press, Cambridge, MA, 1986.
- [8] W. B. Dean, "Linear Least Squares for Correlated Data," 10<sup>th</sup> Annual International Conference of the International Society of Parametric Analysis, 1988.
- [9] Polynomial regression From Wikipedia.  
[http://en.wikipedia.org/wiki/Polynomial\\_regression](http://en.wikipedia.org/wiki/Polynomial_regression).
- [10] N. Y. Ermolova, "Spectral Analysis of Nonlinear Amplifier Based on the Complex Gain Taylor Series Expansion," IEEE Communications Letters, Vol. 5, No. 12, Dec. 2001.